Indonesian Journal of Pharmacy

VOL 37 (2) 2026: 299–311| RESEARCH ARTICLE

Redox-Driven Stability and Synergism of Glabridin and Proanthocyanidin Nanoparticles

Pimporn Anantaworasakul[1], Puttaporn Sriwattanachai[1], Ratiporn Palee[1] and Chuda Chittasupho[1]*

Department of Pharmaceutical Sciences, Faculty of Pharmacy, Chiang Mai University, Mueang, Chiang Mai 50200, Thailand

Article Info

Submitted: 09-02-2026
Revised: 10-04-2026
Accepted: 13-04-2026

*Corresponding author
Chuda Chittasupho

Email:
chuda.c@cmu.ac.th

ABSTRACT

This study aimed to develop and characterize phosphatidylcholine-based nanoparticles encapsulating proanthocyanidin and glabridin, two natural polyphenolic antioxidants. Nanoparticles were prepared by the solvent-displacement method and characterized for particle size, polydispersity index (PDI), zeta potential, encapsulation efficiency, and *in vitro* release. Antioxidant activity was evaluated using DPPH, ABTS, and FRAP assays, and physical and chemical stability was assessed during storage at 4°C and 30°C for four weeks. The prepared glabridin and proanthocyanidin nanoparticles exhibited mean sizes of 85.42 ± 3.29 nm and 159.47 ± 4.47 nm, with encapsulation efficiencies of 49.73 ± 0.72% and 89.48 ± 4.57%, respectively. Both formulations demonstrated a biphasic release profile and improved antioxidant activity compared to their free forms. Notably, a mixture of glabridin and proanthocyanidin nanoparticles at a ratio of 2:1 exhibited the highest ferric-reducing antioxidant power (FRAP), suggesting enhanced reducing activity and potential interaction between the two antioxidants. Stability studies revealed that 4°C storage effectively preserved particle integrity, antioxidant activity, and compound content, whereas 30°C accelerated degradation and reduced scavenging capacity. These findings suggest that nanoencapsulation may improve the solubility and stability of poorly water-soluble antioxidants, thereby enhancing antioxidant performance. This combined nanoparticle system may have potential for applications related to oxidative stress mitigation.

Keywords: drug delivery; proanthocyanidin; glabridin; antioxidant; nanoparticles

INTRODUCTION

Oxidative stress, resulting from an imbalance between reactive oxygen species (ROS) and the antioxidant defense system, plays a pivotal role in the pathogenesis of numerous chronic diseases, including neurodegenerative disorders, cardiovascular diseases, and inflammation (Dash et al., 2025; Garcia-Llorens et al., 2025; Reddy, 2023). Polyphenolic antioxidants have gained significant attention for their ability to neutralize free radicals and prevent oxidative damage via hydrogen-atom or electron-donation mechanisms (Ahmad et al., 2025). In addition to their strong free-radical-quenching properties, both compounds demonstrate notable anti-inflammatory and neuroprotective effects, supporting their therapeutic potential in oxidative stress–related disorders.

Glabridin is a lipophilic isoflavan with strong biological activity, but its application is limited by poor water solubility and low bioavailability, which restrict effective delivery in biological systems (Ciupei et al., 2024; Zhang et al., 2023). In free form, glabridin is gradually depleted during redox reactions and shows limited capacity to sustain antioxidant activity over time (Choi et al., 2021). Proanthocyanidins are water-soluble, polymeric polyphenols with high intrinsic antioxidant capacity; however, their high molecular weight and polymeric structure limit membrane permeability and bioavailability. They are also prone to oxidation, aggregation, and nonspecific interactions with biomolecules, leading to rapid consumption and reduced sustained antioxidant activity (Li et al., 2026).

Moreover, when administered in free form, phenolic antioxidants are rapidly depleted during radical scavenging and often fail to sustain activity over time (Chandimali et al., 2025). This has prompted interest in antioxidant regeneration mechanisms, in which certain antioxidants can be recycled or regenerated through redox interactions with complementary compounds, thereby extending their efficacy. Co-delivery of phenolics with differing redox potentials may further enhance this effect through synergistic regeneration. Nanoparticle-based delivery systems, particularly those composed of phospholipids such as phosphatidylcholine, offer a promising approach to overcome these challenges (Patel et al., 2024). Nanoparticles improve antioxidant performance by enhancing solubility, protecting labile compounds from degradation, and facilitating controlled release (Thiruvengadam et al., 2025). Additionally, the spatial organization and partitioning of antioxidants within nanoparticles may promote interactions at the oil–water interface, favoring redox cycling and synergistic antioxidant effects (Farooq et al., 2021).

However, despite increasing interest in nanoparticle-based delivery of polyphenols, most studies have focused on single-compound systems, while the combined behavior of structurally distinct antioxidants within nanoparticle formulations remains insufficiently explored. In particular, the potential interactions between lipophilic and hydrophilic polyphenols, such as glabridin and proanthocyanidin, and their impact on antioxidant performance and stability have not been clearly elucidated. Therefore, this study aimed to develop and characterize phosphatidylcholine-based nanoparticles containing glabridin and proanthocyanidin, and to evaluate their individual and combined antioxidant activities using DPPH, ABTS, and FRAP assays. In addition, the stability of the nanoparticle systems was investigated under different storage conditions (4°C and 30°C). This work provides insight into the behavior of combined antioxidant systems in nanoparticle formulations and their potential for improving antioxidant performance.

MATERIALS AND METHODS

Materials

2,2-Diphenyl-1-picrylhydrazyl (DPPH) (≥98.0%), 2,4,6-Tripyridyl-s-Triazine (TPTZ) (≥99.0%), and 2,2'-Azino-bis(3-ethylbenzothiazoline-6-sulfonic acid) (ABTS) were obtained from Sigma-Aldrich, St. Louis, MO, USA. Phosphatidylcholine (90%), Epigallocatechin gallate (EGCG, 98%), Ascorbic acid, Cholesterol, Glabridin, Poloxamer 407, and Proanthocyanidin were purchased from MyskinRecipes, Bangkok, Thailand. Ethanol (95%) and acetone were sourced from World Chemical, Chiang Mai, Thailand, while ethanol (99.8%) was obtained from RCI Labscan, Bangkok, Thailand. Potassium persulfate (98%) and Ferrous sulfate heptahydrate ($FeSO_4 \bullet 7H_2O$, 99%) were procured from Loba Chemie, India. Ferric chloride hexahydrate ($FeCl_3 \bullet 6H_2O$, 99%) was obtained from QReC, New Zealand.

Methods

Preparation of Proanthocyanidin and Glabridin Nanoparticles Using Solvent Displacement Technique

For the preparation of proanthocyanidin nanoparticles, the organic phase consisted of 1000 µL of proanthocyanidin solution (5 mg/mL), 2000 µL of phosphatidylcholine solution (15 mg/mL), and 200 µL of cholesterol solution in acetone (10 mg/mL). For the preparation of glabridin nanoparticles, the organic phase consisted of 1000 µL of glabridin solution (10 mg/mL), 2000 µL of phosphatidylcholine solution (15 mg/mL), and 200 µL of cholesterol solution in acetone (10 mg/mL). The aqueous phase was prepared by mixing 13,350 µL of ultrapure water, 1500 µL of 1% poloxamer, and 150 µL of polyethylene glycol (PEG) using a vortex mixer, resulting in a total volume of 15 mL. The organic phase was then injected dropwise into the aqueous phase under continuous stirring at 800 rpm using a magnetic stirrer. Ethanol was removed from the nanoparticle suspension by stirring at 800 rpm for 12 hours. The proanthocyanidin and glabridin nanoparticles obtained were characterized for subsequent analysis.

Characterization of Proanthocyanidin and Glabridin Nanoparticles

Particle Size, Polydispersity Index (PDI), and Zeta Potential Analysis

The nanoparticle suspension was pipetted into a folded capillary zeta cell, and the particle size, PDI, and zeta potential were measured using a zetasizer (Malvern, UK). The experiments were performed in triplicate, and the average values were recorded.

Encapsulation Efficiency (%EE) of Proanthocyanidin and Glabridin Nanoparticles

The standard curves for proanthocyanidin and glabridin were established by dissolving 10 mg of proanthocyanidin in dimethyl sulfoxide (DMSO),

followed by serial dilution to obtain a range of concentrations. The absorbance was measured at 300 nm using a microplate reader (Spectramax M3, Thermo Scientific, Waltham, MA, USA), and a standard curve was constructed. Encapsulation efficiency (%EE) was determined using a direct method by measuring the total amount of compound present in the nanoparticle dispersion. The nanoparticle samples were appropriately diluted, and the absorbance was measured at 300 nm using a microplate reader (Spectramax M3, Thermo Scientific, Waltham, MA, USA). The measured absorbance values were corrected by subtracting the corresponding blank nanoparticle formulation (without active compound) to minimize interference from formulation components. The concentration of the compound in the nanoparticles was then calculated using the standard calibration curves.

$$\%EE = \frac{Amount\ of\ compound\ in\ NPs}{Amount\ of\ compound\ initially\ added} x\ 100\%$$

In Vitro Release Study in Phosphate Buffered Saline (PBS)

The release of proanthocyanidin and glabridin from nanoparticles was evaluated using a Transwell® system. A 200 µL aliquot of nanoparticle suspension was placed into the Transwell® chamber, while 1 mL of phosphate-buffered saline (PBS) at pH 7.4 was added to the outer chamber (Chittasupho et al., 2023). The system was incubated at 37°C, and at predefined time intervals (1, 2, 18, 24, 48, 72, 96, and 120 h), 50 µL of the sample was withdrawn and replaced with fresh PBS. The withdrawn samples were mixed with 50 µL of DMSO, and the absorbance was measured at 300 nm (Spectramax M3, Thermo Scientific, Waltham, MA, USA) to determine cumulative drug release.

Preparation of Nanoparticle Combinations

Glabridin and proanthocyanidin nano-particles were mixed in different ratios (2:1, 1:1, and 1:2) using a vortex mixer to obtain nanoparticle combinations for subsequent studies.

Antioxidant Activity Evaluation

DPPH Radical Scavenging Assay

Antioxidant activity was assessed using the DPPH radical-scavenging assay. A 500 µM DPPH solution was prepared in absolute ethanol. Test samples (100 µL) were pipetted into a 96-well plate, followed by the addition of 100 µL of DPPH solution. The mixture was incubated in the dark at room temperature for 30 minutes, and absorbance was measured at 517 nm (Spectramax M3, Thermo Scientific, Waltham, MA, USA). The percentage inhibition of DPPH radicals was calculated.

$$\%Inhibition = \frac{A_{control} - A_{sample}}{A_{control}}\ x\ 100\%$$

ABTS Radical Scavenging Assay

The ABTS radical-scavenging activity was evaluated by preparing an ABTS•+ solution by reacting 7 mM ABTS with 2.45 mM potassium persulfate, which was incubated in the dark for 18 hours. A 20 µL aliquot of the test sample was pipetted into a 96-well plate, followed by the addition of 180 µL of ABTS•+ solution. After 15 minutes of incubation in the dark at room temperature, the absorbance was measured at 734 nm (Spectramax M3, Thermo Scientific, Waltham, MA, USA), and the percentage inhibition of ABTS radicals was calculated.

$$\%Inhibition = \frac{A_{control} - A_{sample}}{A_{control}}\ x\ 100\%$$

Ferric Reducing Antioxidant Power (FRAP) Assay

The FRAP assay was performed by preparing the FRAP reagent consisting of acetate buffer, $FeCl_3$, and 2,4,6-tripyridyl-S-triazine (TPTZ). A 20 µL aliquot of the test sample was mixed with 180 µL of FRAP reagent in a 96-well plate and incubated at 37°C for 30 minutes. Absorbance was measured at 595 nm (Spectramax M3, Thermo Scientific, Waltham, MA, USA). A calibration curve was constructed using ferrous sulfate ($FeSO_4 \cdot 7H_2O$) at concentrations ranging from 0 to 5,000 µM. The FRAP values of the samples were calculated from the standard curve and expressed as micromolar of Fe^{2+}equivalent. All experiments were performed in triplicate, and results were reported as mean ± standard deviation.

Stability Evaluation of Nanoparticles

Physical Stability

The physical stability of nanoparticles was assessed by storing the samples at 4°C and 30°C for up to 4 weeks. At different time points, particle size, PDI, and zeta potential were measured to evaluate stability.

Chemical Stability

The chemical stability of nanoparticles was assessed by storing the samples at 4°C and 30°C and measuring proanthocyanidin and glabridin content using a microplate reader at 300 nm

(Spectramax M3, Thermo Scientific, Waltham, MA, USA) after 2 and 4 weeks of storage.

Statistical analysis

The data were analyzed using GraphPad Prism 8 (La Jolla, CA, USA) using two-way analysis of variance (ANOVA) to evaluate the effects of temperature and time, followed by Tukey's post hoc test for multiple comparisons. A p-value of less than 0.05 was considered statistically significant.

RESULTS AND DISCUSSION

Characterization of Proanthocyanidin and Glabridin Nanoparticles

The stability of glabridin and proanthocyanidin nanoparticles was assessed over four weeks by monitoring particle size, polydispersity index (PDI), and zeta potential at 4°C and 30°C (Figure 1). The results indicate that storage temperature significantly affects the stability of both nanoparticle types, with 30°C promoting aggregation and size increase, particularly for proanthocyanidin nanoparticles.

The particle size of glabridin nanoparticles remained relatively stable at 4°C, with only a minor increase over time. However, at 30°C, a significant increase in size was observed after 2 and 4 weeks. In contrast, proanthocyanidin nanoparticles exhibited a more pronounced increase in size at 30°C, reaching over 200 nm after 2 and 4 weeks. These results suggest that proanthocyanidin nanoparticles are more sensitive to temperature variations, making 4°C a more suitable storage condition to maintain their stability.

The polydispersity index (PDI), which reflects the uniformity of nanoparticle size distribution, exhibited distinct trends across formulations. Glabridin nanoparticles maintained a relatively low and stable PDI at both temperatures, suggesting good colloidal stability. A slight decrease in PDI at 30°C was observed at weeks 2 and 4, indicating a narrower particle size distribution under these conditions. In contrast, proanthocyanidin nanoparticles showed a significant increase in PDI at 30°C, at weeks 2 and 4, indicating increased size heterogeneity and possible particle size instability. At 4°C, PDI remained stable, further supporting the better stability of proanthocyanidin nanoparticles under lower temperatures. The zeta potential, which represents surface charge and stability, was also evaluated over time. Glabridin nanoparticles showed only minor changes in zeta potential, with no significant differences between 4°C and 30°C, except for a slight increase after 2 weeks. This suggests that glabridin nanoparticles maintained sufficient electrostatic repulsion to prevent aggregation. Proanthocyanidin nanoparticles, however, exhibited a significant increase in zeta potential (more negative) at 30°C by week 2 and week 4, possibly due to the presence of the ionized form of proanthocyanidin on the surface of the nanoparticles.

Encapsulation Efficiency of Proanthocyanidin and Glabridin Nanoparticles

Encapsulation efficiency (%EE) was evaluated using a microplate reader at 300 nm. The results indicated that proanthocyanidin nanoparticles exhibited a higher %EE (89.48 ± 4.57%) compared to glabridin nanoparticles (49.73 ± 0.72%). This suggests that proanthocyanidin was more effectively encapsulated within the nanoparticle matrix, whereas glabridin exhibited moderate encapsulation efficiency.

***In Vitro* Drug Release Study**

The cumulative release of glabridin and proanthocyanidin nanoparticles was evaluated over 120 hours to assess their drug-release behavior (Figure 2). The release profiles demonstrate a biphasic pattern, characterized by an initial burst release followed by a sustained release phase. Within the first 24 hours, both nanoparticle types exhibited rapid initial release, with glabridin nanoparticles releasing approximately 57.05±11.32% of the encapsulated compound, whereas proanthocyanidin nanoparticles released approximately 43.08±4.11%. This initial burst may be attributed to the release of surface-adsorbed drug molecules that were loosely bound to the nanoparticle matrix. Followingthe burst phase, the release rate decreased, indicating a controlled, sustained release mechanism. By 120 hours, glabridin nanoparticles exhibited a cumulative release of nearly 100%, whereas proanthocyanidin nanoparticles reached approximately 60%. This difference suggests that glabridin nanoparticles release their payload more rapidly, while proanthocyanidin nanoparticles provide a more prolonged release, potentially due to stronger interactions between proanthocyanidin and the nanoparticle matrix. The sustained release observed in both formulations is beneficial for extended drug retention, reducing the need for frequent administration.

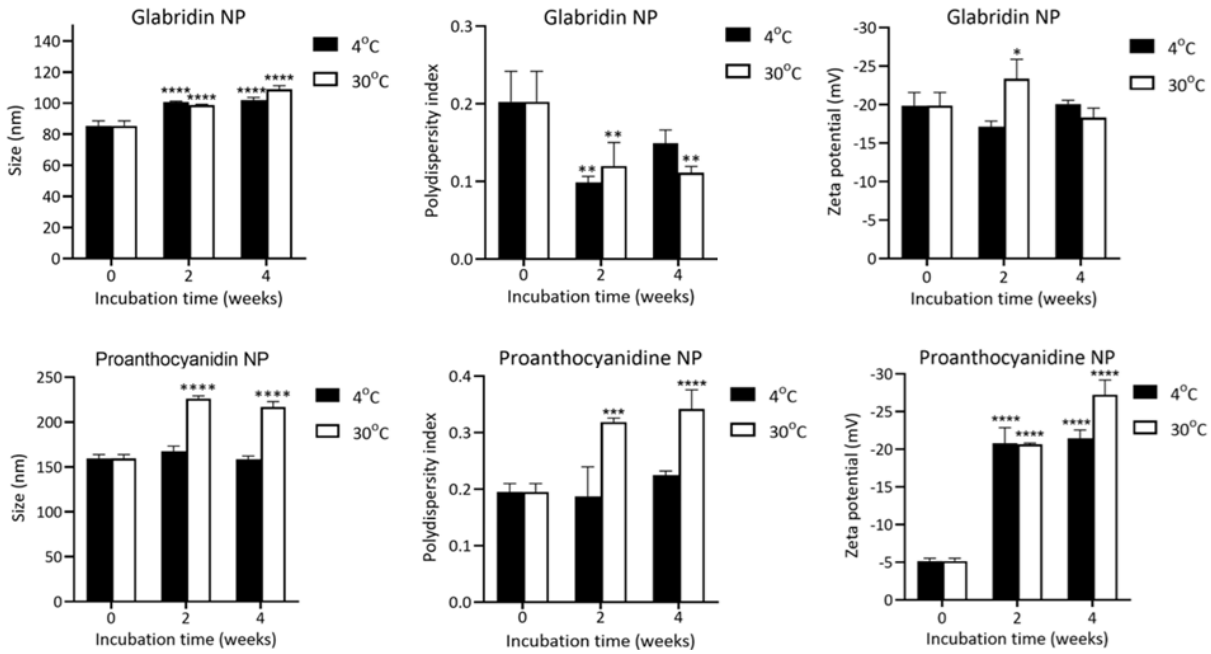

Figure 1. Particle size, polydispersity index (PDI) values, and zeta potential values of glabridin nanoparticles (Glabridin NP) and proantho-cyanidin nanoparticles (Proanthocyanidin NP) stored at 4°C and 30°C over different time points. Data are presented as mean ± standard deviation. *, **, ***, and **** indicate $p<0.05$, $p<0.01$, $p<0.001$, and $p<0.0001$, respectively.

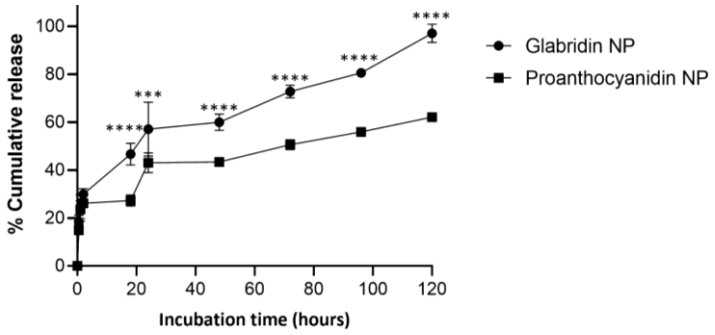

Figure 2. Release profiles of nanoparticles containing glabridin and proanthocyanidin in phosphate-buffered saline (PBS) at pH 7.4 over 120 hours. The cumulative release percentage was measured at various time points and plotted as mean ± standard deviation. Statistical significance relative to hour 0 is indicated by *** ($p < 0.001$) and **** ($p < 0.0001$).

This controlled-release behavior suggests that nanoparticle encapsulation enhances the solubility and stability of glabridin and proanthocyanidin, making them promising candidates for sustained antioxidant and therapeutic applications.

Antioxidant Activity of Proanthocyanidin and Glabridin Nanoparticles

The antioxidant activities of glabridin and proanthocyanidin, both in their pure forms and as nanoparticle formulations, were compared using DPPH, ABTS, and FRAP assays (Figure 3). The IC_{50} values revealed significant differences in activity depending on the compound form and the assay used. In the DPPH assay, which measures the ability to neutralize free radicals, the pure form of glabridin (2205±357 μg/mL) exhibited significantly lower antioxidant activity than its nanoparticle formulation (836±84 μg/mL). The pure form of proanthocyanidin (317±42 μg/mL)

showed significantly higher antioxidant potency compared with proanthocyanidin nanoparticles (851.8±311 µg/mL), which may be attributed to differences in release kinetics and accessibility of the active compound. The *in vitro* release study demonstrated that glabridin nanoparticles exhibited a faster and more extensive release profile, whereas proanthocyanidin nanoparticles showed a slower and more sustained release (~60% at 120 h). This sustained-release behavior may limit the immediate availability of proanthocyanidin to interact with DPPH radicals, leading to a higher apparent IC_{50} value.

The IC_{50} values of the reference antioxidants, including EGCG and ascorbic acid, were found to be 65.69±12 µg/mL and 132.4±13 µg/mL, respectively. The enhanced antioxidant activity of glabridin nanoparticles is likely due to increased surface area and solubility, which facilitate better interaction with free radicals.

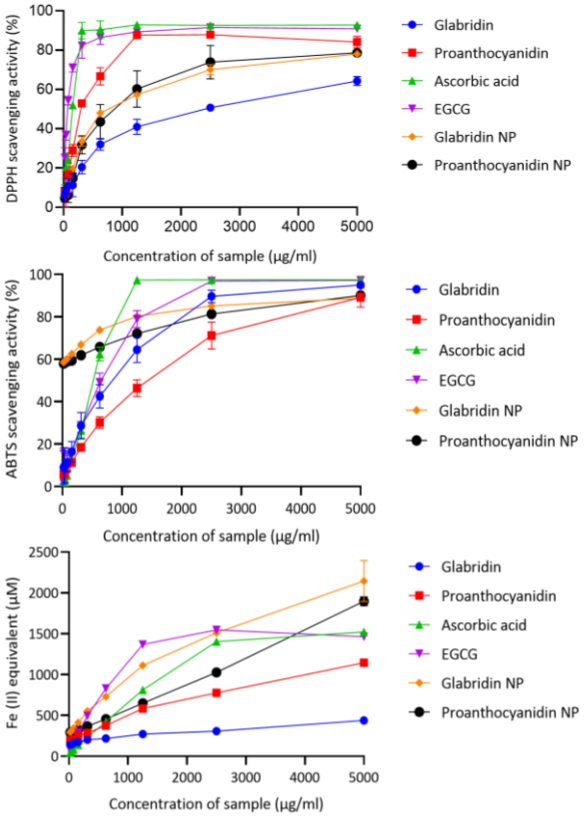

Figure 3. DPPH and ABTS radical-scavenging activities and ferric-reducing capacity of different samples at various concentrations. Data are presented as mean ± standard deviation.

In contrast, the ABTS assay revealed a distinct antioxidant profile. Glabridin nanoparticles and proanthocyanidin nanoparticles showed remarkably strong ABTS radical scavenging activity, with very low IC_{50} values of 12.41 and 13.94 µg/mL, respectively. Among the free compounds, glabridin (670.9 µg/mL), EGCG (566.3 µg/mL), and ascorbic acid (472.1 µg/mL) demonstrated moderate activity, while proanthocyanidin exhibited the weakest ABTS scavenging effect (IC_{50} = 1197 µg/mL). This substantial enhancement in ABTS free radical scavenging activities suggests that nanoencapsulation significantly improves the compounds' accessibility to aqueous-phase radicals, possibly by increasing dispersion and reactivity in hydrophilic environments.

Glabridin nanoparticles and proanthocyanidin nanoparticles demonstrated superior ferric reducing activity, with FRAP values of 2144.33 and 1897.58 µM, respectively. These were substantially higher than those of their pure forms, i.e., glabridin (439.32 µM) and proanthocyanidin (1143.78 µM), indicating enhanced electron-donating capacity. While EGCG and ascorbic acid also showed strong reducing power (1463.23 and 1522.51 µM), the nanoparticle formulations exceeded their activity, suggesting that nanoencapsulation not only preserved but also enhanced redox potential.

Stability of Proanthocyanidin and Glabridin Nanoparticles

Chemical Stability

The chemical stability of nanoparticles was evaluated by measuring the remaining percentage of glabridin and proanthocyanidin in the formulations over 4 weeks. A significant decline in the remaining percentage was observed for glabridin nanoparticles stored at both temperatures, suggesting degradation. Proanthocyanidin nanoparticles remained stable for 2 weeks but exhibited significant degradation at 4 weeks. These findings suggest that proanthocyanidin nanoparticles have better chemical stability than glabridin nanoparticles, likely due to proanthocyanidin's inherent antioxidant properties.

The stability study of glabridin-loaded nanoparticles showed a time-dependent decline in the remaining glabridin content, with more pronounced degradation at 30°C than at 4°C.

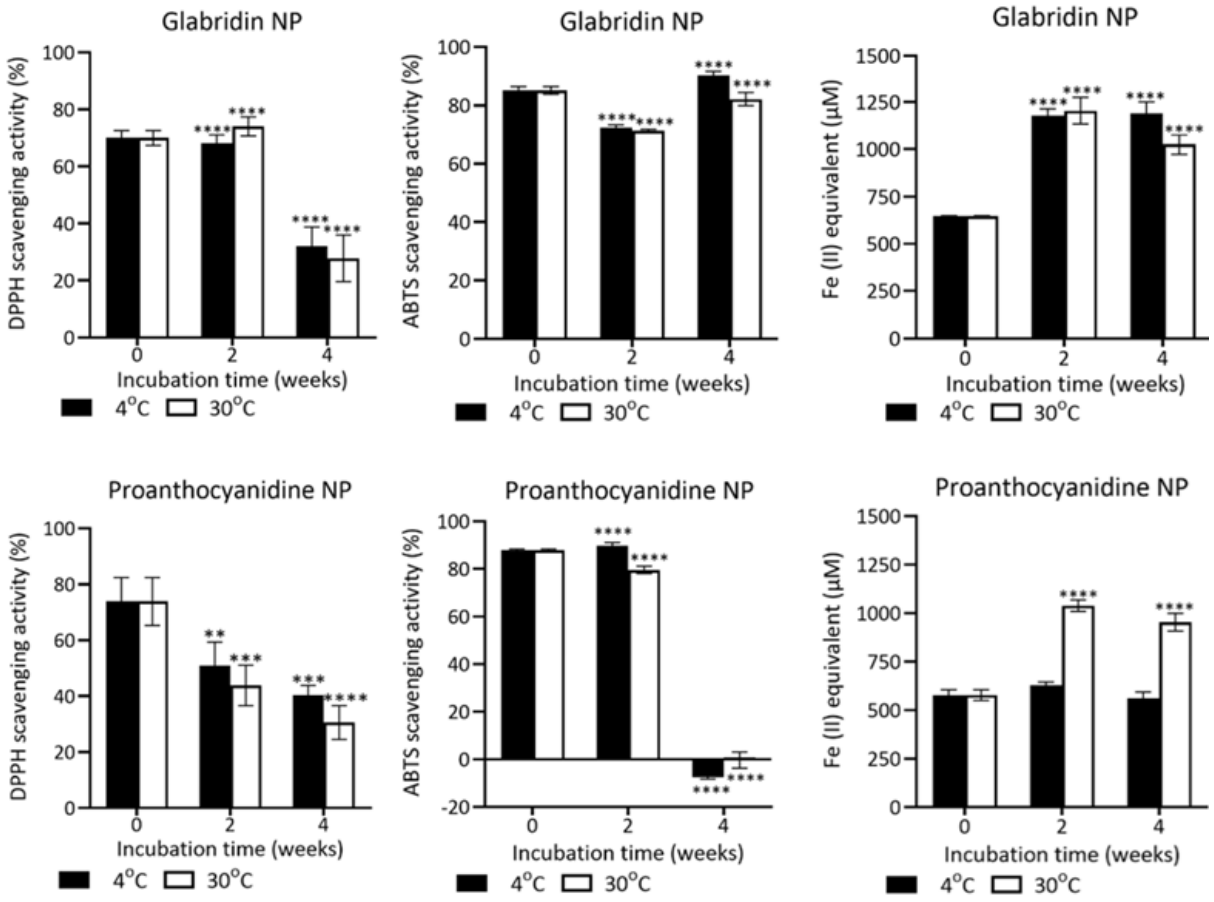

Figure 4. The DPPH and ABTS radical-scavenging activities and ferric-reducing power of glabridin and proanthocyanidin nanoparticles after storage at 4°C and 30°C for 2 and 4 weeks. Data are presented as mean ± standard deviation. Statistical significance relative to week 0 is indicated by *** ($p < 0.001$) and **** ($p < 0.0001$).

At 4°C, the percentage of glabridin retained was 55.67±2.97% at week 2 and 45.56±2.89% at week 4, indicating a gradual reduction in stability. In contrast, storage at 30°C resulted in a faster decline, with only 51.47±1.50% remaining at week 2 and 32.63±1.09% at week 4. These findings confirm that lower temperatures enhance the stability of glabridin in nanoparticles, significantly slowing down its degradation compared to ambient conditions.

The stability study of proanthocyanidin-loaded nanoparticles at 4°C and 30°C showed a time-dependent reduction in proanthocyanidin content at both temperatures. At 4°C, the retained proanthocyanidin content was 95.13 ± 6.96% at week 2 but decreased markedly to 39.56 ± 0.80% by week 4, indicating a substantial decline during the later storage period. At 30°C, 99.32 ± 1.03% remained at week 2 and decreased to 61.04 ± 0.84% at week 4. Overall, the results indicate that degradation occurred at both temperatures, with lower remaining content observed at 4°C than at 30°C, at week 4.

Stability of Antioxidant Activity

The DPPH radical scavenging activity of glabridin nanoparticles and proanthocyanidin nanoparticles over a 4-week storage period at two different temperatures: 4°C and 30°C (Figure 4). For glabridin nanoparticles, DPPH scavenging activity increased slightly at week 2, reaching approximately 80% at both storage temperatures. However, by week 4, activity had declined to approximately 40% at 4°C and slightly lower at 30°C. These results corresponded well with the %remaining of glabridin in nanoparticles, which were 45.6% and 32.6%, when stored at 4°C and 30° C, respectively. The drop in activity suggests time-

dependent degradation of the antioxidant components, though the storage temperature did not appear to significantly influence the extent of degradation at this later time point.

The ABTS scavenging activity remained relatively high throughout the 4-week period. A slight but statistically significant decrease was observed at week 2, dropping to approximately 75% for both temperatures. By week 4, activity remained stable, with no further significant loss, indicating that glabridin nanoparticles retained good antioxidant stability under both refrigerated and room-temperature conditions. The minimal changes over time suggest that glabridin nanoparticles are relatively stable with respect to their ABTS radical-scavenging activity, and that storage temperature had a limited effect on their performance.

In contrast, proanthocyanidin nanoparticles exhibited a steady, more pronounced decline in antioxidant activity over time. At week 2, the DPPH scavenging ability dropped to approximately 50–55%, with a sharper reduction observed at 30°C. By week 4, the activity further decreased to about 40% at 4°C and around 30% at 30°C.

For ABTS scavenging activity, a moderate decline was observed by week 2, decreasing to approximately 80% at 4 °C and 75% at 30 °C. By week 4, a marked and statistically significant reduction in antioxidant activity was observed. The ABTS scavenging values became negative, particularly at 4 °C, indicating a substantial loss of measurable antioxidant capacity. This pronounced decrease is consistent with the concurrent reduction in proanthocyanidin content and DPPH radical-scavenging activity during storage, suggesting that degradation or transformation of the active compounds contributed to the diminished activity. However, it may also be influenced by assay-related limitations. The ABTS assay is highly sensitive to reaction conditions, and factors such as solvent system, pH, and changes in sample composition during storage (e.g., degradation products or matrix alterations) can affect absorbance-based measurements (Wolosiak et al., 2022; Zheng et al., 2016). Therefore, the negative values are more appropriately interpreted as a combination of substantial loss of antioxidant activity and potential analytical interference.

For glabridin nanoparticles, the initial FRAP value at week 0 was approximately 650 μM for both storage conditions, indicating moderate baseline reducing activity. At week 2, a significant increase was observed, with Fe(II) equivalents rising to approximately 1200 μM at both temperatures. This enhanced reducing power was maintained through week 4, although a slight reduction was seen at 30°C compared to 4°C. The sustained high FRAP values suggest good oxidative stability of glabridin nanoparticles under both storage conditions, with refrigeration slightly better preserving activity. The notable increase from baseline may indicate the release of glabridin and proanthocyanidin from the nanoparticle matrix over time, which enhanced the exposure or availability of redox-active groups.

In contrast, proanthocyanidin nanoparticles exhibited a different stability profile. At week 2, a significant divergence between temperatures was observed. The reducing power increased substantially at 30°C, reaching over 1000 μM, whereas the activity remained unchanged at 4°C. A similar pattern persisted at week 4, with the 30°C group maintaining high reducing capacity (~950 μM) and the 4°C group showing minimal change.

This suggests that proanthocyanidin nanoparticles may undergo temperature-dependent transformation, potentially enhancing their reducing power at ambient temperature. However, the concurrent decline in radical-scavenging activity (as evidenced by ABTS and DPPH data) suggests that these changes may involve degradation processes that release phenolic or redox-active fragments.

Antioxidant activity of Glabridin and Proanthocyanidin Nanoparticle mixture

The antioxidant activity of glabridin and proanthocyanidin nanoparticles, as well as their combinations in different ratios (2:1, 1:1, and 1:2), was assessed using DPPH, ABTS, and FRAP assays (Figure 5).

The DPPH and ABTS assays demonstrated that the free radical-scavenging potential correlated with the proportion of glabridin nanoparticles.

The FRAP assay indicated that glabridin and proanthocyanidin nanoparticles showed comparable reducing power, with no significant difference. The combination ratios among the different formulations showed a significant alteration in their activity. In particular, the mixture of a 2:1 glabridin-to-proanthocyanidin nanoparticles ratio showed the highest reducing activity. This result might indicate a synergistic effect on ferric-reducing antioxidant power.

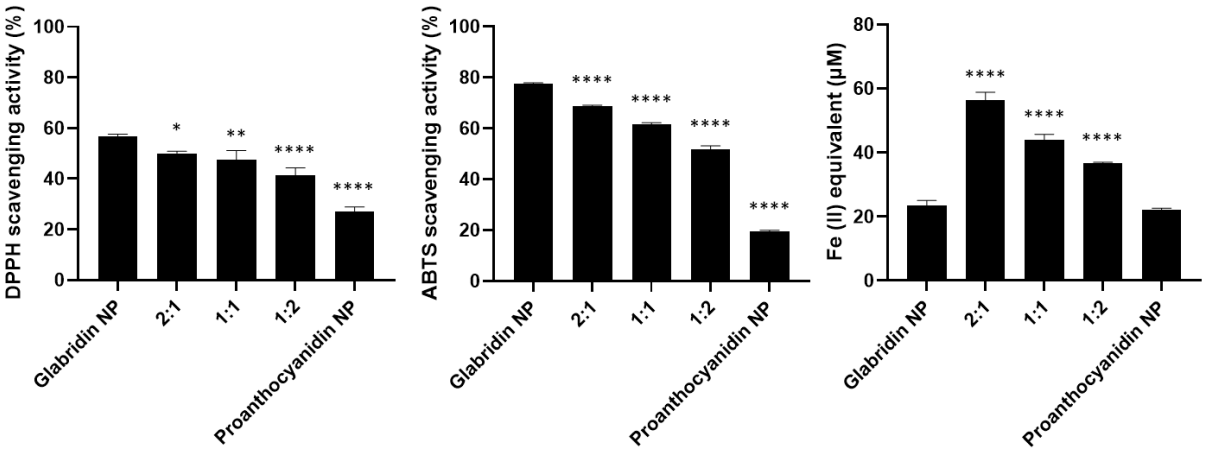

Figure 5. The DPPH and ABTS radical-scavenging activities and ferric-reducing power of various nanoparticle formulations, including glabridin and proanthocyanidin nanoparticle mixtures at ratios of 2:1, 1:1, and 1:2, as well as individual proanthocyanidin and glabridin nanoparticles. Data are presented as mean ± standard deviation. Statistical significance relative to glabridin nanoparticlesis indicated by *, **, and **** indicate $p<0.05$, $p<0.01$, and $p<0.0001$, respectively

Discussion

In this study, proanthocyanidin and glabridin nanoparticles were successfully prepared via the solvent-displacement method. Glabridin, a lipophilic isoflavan, interacts strongly with phosphatidylcholine through dominant hydrophobic insertion into the lipid acyl-chain region, supported by hydrogen bonding between its phenolic hydroxyl groups and phospholipid carbonyl and phosphate moieties (Zhang et al., 2021). This molecular association localizes glabridin primarily within the hydrophobic core and interfacial regions of phosphatidylcholine-based lipid nanoparticles, resulting in high encapsulation efficiency, reduced burst release, and enhanced physicochemical stability (Lin et al., 2024). The interaction resembles a phospholipid–drug complex rather than simple surface adsorption, accounting for the improved bioavailability and sustained biological activity of glabridin-loaded lipid nanoparticles (Patel et al., 2024).

Although proanthocyanidins are hydrophilic, their multiple phenolic hydroxyl groups enable strong hydrogen bonding and interfacial interactions with phosphatidylcholine headgroups (Karonen, 2022). The aromatic rings of proanthocyanidins further stabilize the complex via π–cation interactions with the choline moiety, resulting in predominant localization at the phospholipid headgroup–acyl chain interface (Villalain, 2022). This interfacial trapping restricts molecular mobility, thereby enhancing encapsulation efficiency, improving chemical stability, and sustaining release from phosphatidylcholine-based lipid nanoparticles (Zakharov et al., 2026).

The release profiles of proanthocyanidin and glabridin nanoparticles displayed a biphasic release pattern, characterized by an initial rapid release within the first 24 hours, followed by a slower, sustained release. The initial burst release was attributed to surface-adsorbed proanthocyanidin and glabridin. The subsequent sustained release phase resulted from the gradual diffusion of encapsulated compounds through the nanoparticle matrix.

Antioxidant activity was assessed using the DPPH, ABTS, and FRAP assays, revealing formulation-dependent differences between free and nanoparticle forms. For glabridin, the nanoparticle formulation showed improved antioxidant activity compared with the free compound, as reflected by a lower IC_{50} value in the DPPH assay. This improvement may be associated with enhanced dispersion and apparent solubility of the lipophilic compound within the nanoparticle system, facilitating better interaction with free radicals (Yu et al., 2022). In contrast, for proanthocyanidin, although the nanoparticle formulation exhibited a numerically higher IC_{50} value than the free form, this difference was not

statistically significant. This suggests that nanoparticle incorporation did not substantially alter the DPPH radical-scavenging activity of proanthocyanidin under the conditions tested.

Glabridin- and proanthocyanidin-loaded nanoparticles exhibited effective DPPH and ABTS radical scavenging due to hydrogen atom and electron donation from phenolic hydroxyl groups. However, during storage at 30°C, proanthocyanidin nanoparticles exhibited a gradual decline in radical-scavenging activity, which may be associated with oxidative consumption of phenolic hydroxyl groups, formation of quinone structures, and polymerization-induced masking of reactive sites (Huynh et al., 2026). These structural changes preferentially impair hydrogen-atom transfer–based radical scavenging, whereas electron-transfer capacity may remain partially preserved.

This interpretation is consistent with the observed divergence between radical-scavenging assays (DPPH and ABTS) and FRAP results. While DPPH and ABTS activities decreased during storage, FRAP values increased under certain conditions, suggesting that degradation or transformation of proanthocyanidin may generate smaller phenolic or redox-active species that retain or enhance electron-donating capacity (Souza et al., 2023). In addition, sustained release from the nanoparticle matrix may further increase the availability of redox-active components. Therefore, the antioxidant behavior during storage likely reflects a combination of structural transformation and changes in compound accessibility.

Chemical stability testing showed decreased retention of both glabridin and proanthocyanidin in the nanoparticle formulations after four weeks of storage, indicating some degree of degradation. The degradation of glabridin was likely due to hydrolysis in the aqueous environment, as water is a strong ionizing agent that can reduce glabridin stability (Ao et al., 2010). Similarly, proanthocyanidin is prone to oxidative degradation upon exposure to oxygen (Liang et al., 2024). Alternatively, the observed decrease in compound retention could be attributed to the gradual release of the active compounds into the storage medium. The stability of antioxidant activity was also evaluated, revealing a decrease in DPPH and ABTS scavenging activity after two weeks of storage, likely due to the degradation of active compounds.

The enhanced antioxidant activity observed in the nanoparticle formulations may be further understood in light of redox cycling and antioxidant regeneration mechanisms. According to the previous study, antioxidants with lower redox potentials (E°) are thermodynamically capable of reducing oxidized antioxidant radicals back to their active forms (Decker et al., 2010). In this study, EGCG and ascorbic acid demonstrated strong antioxidant activity in all assays due to their low E° values (~282–430 mV), which enable effective hydrogen or electron donation. Similarly, both proanthocyanidin and glabridin, as polyphenolic compounds, are likely to undergo redox reactions that enable regeneration or recycling during radical scavenging. (Lee et al., 2015; Rumpf et al., 2023; Wolosiak et al., 2022)

The observed increase in FRAP values with storage time, particularly for glabridin nanoparticles, suggests enhanced electron-donating capacity, possibly due to the formation of redox-active degradation products or rearrangements of the nanoparticle matrix that increase accessibility to reducing moieties. This is consistent with the antioxidant regeneration theory, in which oxidized antioxidants can be converted back to their active forms in the presence of other redox-active compounds or favorable matrix environments (Razzak et al., 2019).

Interestingly, the combination of glabridin and proanthocyanidin nanoparticles at a 2:1 ratio exhibited the highest FRAP values, potentially indicating synergistic antioxidant interactions, including via redox cycling. Although a formal regeneration mechanism was not directly measured in this study, the combined system's performance aligns with prior findings in which one antioxidant regenerates another, such as the well-documented ascorbic acid–α-tocopherol system. Although no significant additive or synergistic effects were observed in the DPPH and ABTS assays, the enhanced FRAP activity suggests that redox regeneration between glabridin and proanthocyanidin may be more readily detectable in electron-transfer-based systems than in radical-scavenging assays, where such regeneration may not be kinetically favorable.

Moreover, the improvement in antioxidant activity upon nanoencapsulation can be partially attributed to improved spatial distribution and increased solubility, which facilitate more effective radical scavenging and may enhance redox interactions (Pateiro et al., 2021).

These observations support the hypothesis that nanoencapsulation not only protects antioxidants from degradation but may also

promote intramatrix redox cycling, thereby sustaining or even enhancing antioxidant efficacy over time. Future studies should compare redox potentials and regeneration kinetics among proanthocyanidin, glabridin, and their oxidation products to further validate the possibility of synergistic interactions via antioxidant recycling mechanisms.

CONCLUSION

This study developed phosphatidylcholine-based nanoparticles that encapsulate glabridin and proanthocyanidin, demonstrating enhanced antioxidant activity, controlled release, and improved stability relative to their free forms. The mixture of glabridin and proanthocyanidin nanoparticle formulations exhibited the highest ferric-reducing antioxidant power (FRAP), suggesting potential synergistic antioxidant regeneration via redox cycling. Stability assessments revealed that storage at 4°C preserved antioxidant activity and compound integrity more effectively than storage at 30°C, which accelerated degradation.

ACKNOWLEDGMENTS

The researchers acknowledge the Faculty of Pharmacy, Chiang Mai University, for the equipment and facilities used in this research.

CONFLICT OF INTEREST

The authors declare no conflict of interest.

REFERENCES

Ahmad, Z., Rauf, A., Orhan, I. E., Mubarak, M. S., Akram, Z., Islam, M. R., Imran, M., Edis, Z., Kondapavuluri, B. K., Thangavelu, L., & Thiruvengadam, M. (2025). Antioxidant potential of polyphenolic compounds, sources, extraction, purification, and characterization techniques: A focused review. *Food Science & Nutrition*, *13*(12), e71259. https://doi.org/10.1002/fsn3.71259

Ao, M., Shi, Y., Cui, Y., Guo, W., Wang, J., & Yu, L. (2010). Factors influencing glabridin stability. *Natural product communications*, *5*(12), 1907–1912. https://doi.org/10.1177/1934578X1000501214

Chandimali, N., Bak, S. G., Park, E. H., Lim, H. J., Won, Y. S., Kim, E. K., Park, S. I., & Lee, S. J. (2025). Free radicals and their impact on health and antioxidant defenses: A review. *Cell Death Discovery*, *11*(1), 19. https://doi.org/10.1038/s41420-024-02278-8

Chittasupho, C., Srisawad, K., Arjsri, P., Phongpradist, R., Tingya, W., Ampasavate, C., & Dejkriengkraikul, P. (2023). Targeting spike glycoprotein S1 mediated by NLRP3 inflammasome machinery and the cytokine releases in A549 lung epithelial cells by nanocurcumin. *Pharmaceuticals*, *16*(6), 862. https://doi.org/10.3390/ph16060862

Choi, L. S., Jo, I. G., Kang, K. S., Im, J. H., Kim, J., Kim, J., Chung, J. W., & Yoo, S. K. (2021). Discovery and preclinical efficacy of HSG4112, a synthetic structural analog of glabridin, for the treatment of obesity. *International journal of obesity (2005)*, *45*(1), 130–142. https://doi.org/10.1038/s41366-020-00686-1

Ciupei, D., Colisar, A., Leopold, L., Stanila, A., & Diaconeasa, Z. M. (2024). Polyphenols: From classification to therapeutic potential and bioavailability. *Foods*, *13*(24), 4131. https://doi.org/10.3390/foods13244131

Dash, U. C., Bhol, N. K., Swain, S. K., Samal, R. R., Nayak, P. K., Raina, V., Panda, S. K., Kerry, R. G., Duttaroy, A. K., & Jena, A. B. (2025). Oxidative stress and inflammation in the pathogenesis of neurological disorders: Mechanisms and implications. *Acta pharmaceutica Sinica. B*, *15*(1), 15–34. https://doi.org/10.1016/j.apsb.2024.10.004

Decker, E. A., Elias, R. J., & McClements, D. J. (2010). Oxidation in foods and beverages and antioxidant applications: Understanding mechanisms of oxidation and antioxidant activity. In *Management in Different Industry Sectors* (pp. 321-331). Woodhead Publishing, Cambridge, United Kingdom.

Farooq, S., Abdullah, Zhang, H., & Weiss, J. (2021). A comprehensive review on polarity, partitioning, and interactions of phenolic antioxidants at oil-water interface of food emulsions. *Comprehensive Reviews in Food Science and Food Safety*, *20*(5), 4250-4277. https://doi.org/10.1111/1541-4337.12792

Garcia-Llorens, G., El Ouardi, M., & Valls-Belles, V. (2025). Oxidative stress fundamentals: Unraveling the pathophysiological role of redox imbalance in non-communicable diseases. *Applied Sciences*, *15*(18), 10191. https://doi.org/10.3390/app151810191

Huynh, H. D., Thi, T. H. T., Thi, T. X. T., Nargotra, P., Wang, H. D., Liu, Y. C., & Kuo, C. H. (2026). Recent insights into protein-polyphenol complexes: Molecular mechanisms, processing technologies, synergistic bioactivities, and food applications. *Molecules (Basel, Switzerland)*, *31*(2), 287. https://doi.org/10.3390/molecules31020287

Karonen M. (2022). Insights into polyphenol-lipid interactions: Chemical methods, molecular aspects and their effects on membrane structures. *Plants (Basel, Switzerland)*, *11*(14), 1809. https://doi.org/10.3390/plants11141809

Lee, K. J., Oh, Y. C., Cho, W. K., & Ma, J. Y. (2015). Antioxidant and anti-inflammatory activity determination of one hundred kinds of pure chemical compounds using offline and online screening HPLC assay. *Evidence-based complementary and alternative medicine : eCAM*, *2015*, 165457. https://doi.org/10.1155/2015/165457

Li, Z., Wang, W., Cheng, P., Dong, Q., Chen, H., Fu, K., Fu, C., Pu, Y., & Liu, D. (2026). Proanthocyanidins in food and health: Structure-activity relationships, application challenges, and emerging strategies. *Food chemistry*, *505*, 148067. https://doi.org/10.1016/j.foodchem.2026.148067

Liang, L., Liu, Y., Wu, L., Weng, L., Qiu, H., Zhong, W., & Meng, F. (2024). Advances in extraction protocols, degradation methods, and bioactivities of proanthocyanidins. *Molecules (Basel, Switzerland)*, *29*(10), 2179. https://doi.org/10.3390/molecules29102179

Lin, S., Li, X., Zhang, W., Shu, G., Li, H., Xu, F., Lin, J., Peng, G., Zhang, L., & Fu, H. (2024). Encapsulation nanoarchitectonics of glabridin with sophorolipid micelles for addressing biofilm hazards via extracellular polymeric substance permeation and srtA gene suppression. *Ecotoxicology and environmental safety*, *286*, 117150. https://doi.org/10.1016/j.ecoenv.2024.117150

Patel, P., Garala, K., Singh, S., Prajapati, B. G., & Chittasupho, C. (2024). Lipid-based nanoparticles in delivering bioactive compounds for improving therapeutic efficacy. *Pharmaceuticals (Basel, Switzerland)*, *17*(3), 329. https://doi.org/10.3390/ph17030329

Pateiro, M., Gomez, B., Munekata, P. E. S., Barba, F. J., Putnik, P., Kovacevic, D. B., & Lorenzo, J. M. (2021). Nanoencapsulation of promising bioactive compounds to improve their absorption, stability, functionality and the appearance of the final food products. *Molecules*, *26*(6), 1547. https://doi.org/10.3390/molecules26061547

Razzak, M. A., Lee, J. E., & Choi, S. S. (2019). Structural insights into the binding behavior of isoflavonoid glabridin with human serum albumin. *Food Hydrocolloids*, *91*, 290-300. http://doi.org/10.1016/j.foodhyd.2019.01.031

Reddy, V. P. (2023). Oxidative stress in health and disease. *Biomedicines*, *11*(11), 2925. https://doi.org/10.3390/biomedicines11112925

Rumpf, J., Burger, R., & Schulze, M. (2023). Statistical evaluation of DPPH, ABTS, FRAP, and Folin-Ciocalteu assays to assess the antioxidant capacity of lignins. *International journal of biological macromolecules*, *233*, 123470. https://doi.org/10.1016/j.ijbiomac.2023.123470

Souza, J. N. S., Tolosa, T., Teixeira, B., Moura, F., Silva, E., & Rogez, H. (2023). Optimization of the acid cleavage of proanthocyanidins and other polyphenols extracted from plant matrices. *Molecules*, *28*(1), 66. https://doi.org/10.3390/molecules28010066

Thiruvengadam, R., Kondapavuluri, B. K., Thangavelu, L., Thiruvengadam, M., Hatami, M., & Kim, J. H. (2025). Nanoparticle-based strategies with bioactive compounds for targeting oxidative stress in therapeutic interventions: A comprehensive review. *Industrial Crops and Products*, *227*, 120804. https://doi.org/10.1016/j.indcrop.2025.120804

Villalain J. (2022). Procyanidin C1 location, interaction, and aggregation in two complex biomembranes. *Membranes*, *12*(7), 692. https://doi.org/10.3390/membranes12070692

Wolosiak, R., Drużyńska, B., Derewiaka, D., Piecyk, M., Majewska, E., Ciecierska, M., Worobiej, E., & Pakosz, P. (2022). Verification of the

conditions for determination of antioxidant activity by ABTS and DPPH assays—A practical approach. *Molecules*, *27*(1), 50. https://doi.org/10.3390/molecules27010050

Yu, F., Chen, J., Wei, Z., Zhu, P., Qing, Q., Li, B., Chen, H., Lin, W., Yang, H., Qi, Z., Hong, X., & Chen, X. D. (2022). Preparation of carrier-free astaxanthin nanoparticles with improved antioxidant capacity. *Frontiers in nutrition*, *9*, 1022323. https://doi.org/10.3389/fnut.2022.1022323

Zakharov, A. Y., Berillo, D., Ng, A., Aidarkhanov, D. S., Tukesheva, A. V., Temirkulova, K. M., Tanybayeva, A., Mansurov, Z. A., Balanay, M. P., & Pavlenko, V. V. (2026). Procyanidins: Structural properties, production methods, and modern applications. *Molecules*, *31*(2), 223. https://doi.org/10.3390/molecules31020223

Zhang, C., Lu, Y., Ai, Y., Xu, X., Zhu, S., Zhang, B., Tang, M., Zhang, L., & He, T. (2021). Glabridin liposome ameliorating UVB-induced erythema and lethery skin by suppressing inflammatory cytokine production. *Journal of microbiology and biotechnology*, *31*(4), 630–636. https://doi.org/10.4014/jmb.2011.11006

Zhang, J., Wu, X., Zhong, B., Liao, Q., Wang, X., Xie, Y., & He, X. (2023). Review on the diverse biological effects of glabridin. *Drug Design, Development and Therapy. 17*, 15-37. https://doi.org/10.2147/DDDT.S385981

Zheng, L., Zhao, M., Xiao, C., Zhao, Q., & Su, G. (2016). Practical problems when using ABTS assay to assess the radical-scavenging activity of peptides: Importance of controlling reaction pH and time. *Food chemistry*, *192*, 288–294. https://doi.org/10.1016/j.foodchem.2015.07.015